PHYSICAL REVIEW E **66**, 030501(R) (2002)

Pattern stability and trijunction motion in eutectic solidification

S. Akamatsu,[1] M. Plapp,[2] G. Faivre,[1] and A. Karma[3]
[1]*Groupe de Physique des Solides, CNRS UMR 7588, Universités Denis-Diderot et Pierre-et-Marie-Curie, Tour 23, 2 place Jussieu, 75251 Paris Cedex 05, France*
[2]*Laboratoire de Physique de la Matière Condensée, CNRS/Ecole Polytechnique, 91128 Palaiseau, France*
[3]*Physics Department, Northeastern University, Boston, Massachusetts 02115*
(Received 1 March 2002; published 3 September 2002)

We demonstrate by both experiments and phase-field simulations that lamellar eutectic growth can be stable for a wide range of spacings below the point of minimum undercooling at low velocity, contrary to what is predicted by existing stability analyses. This overstabilization can be explained by relaxing Cahn's assumption that lamellae grow locally normal to the eutectic interface.

DOI: 10.1103/PhysRevE.66.030501 PACS number(s): 64.70.Dv, 81.30.Fb, 05.70.Ln

The solidification of eutectic alloys is both a striking example of spontaneous pattern formation in nature and a metallurgical problem of widely recognized practical importance [1]. This growth process has been traditionally studied by directional solidification experiments where a sample containing a binary alloy of near-eutectic composition is pulled with a fixed speed V in an externally imposed temperature gradient G. This setup produces a wide range of microstructures of which the simplest is an array of lamellae of two coexisting α and β solid phases growing into the metastable liquid, as shown in Fig. 1(a). The steady-state growth of a perfectly periodic lamellar array is described by the classic Jackson-Hunt (JH) theory [2] that predicts the relationship

$$\Delta T(\lambda) \equiv T_E - T_{av}(\lambda) = K_1 V\lambda + K_2/\lambda \tag{1}$$

between the lamellar spacing λ (width of one lamella pair) and the undercooling $\Delta T(\lambda)$ that is the difference between the eutectic temperature T_E, at which the three phases (α, β, and liquid) coexist in equilibrium, and the average temperature of the nonequilibrium eutectic interface spatially averaged over one spacing, $T_{av}(\lambda)$. The first and second terms on the right-hand side of Eq. (1) represent the undercooling necessary to drive the diffusive transport of the two chemical components of the alloy in the liquid (coupled growth) and the capillary undercooling associated with the curvature of the solid-liquid interface, respectively. K_1 and K_2 are constants that only depend on the alloy system and the overall composition of the sample.

The JH result implies that the growth undercooling has a minimum value $\Delta T_m = (4K_1K_2)^{1/2} V^{1/2}$ for a spacing

$$\lambda_m = (K_2/K_1)^{1/2} V^{-1/2}, \tag{2}$$

which is easily found by setting $d\Delta T/d\lambda = 0$.

Lamellar growth is well known to be unstable for spacings smaller than a critical value λ_c. This instability leads to the local elimination of lamellae and is the mechanism by which the array increases its average spacing during the dynamical transient that produces the final pattern. Hence, it is crucially important for understanding pattern selection in this system. Oscillatory instabilities are also known to limit the array stability at large spacing [3,4]. JH have credited Cahn in Ref. [2] for pointing out that λ_c should be equal to λ_m if one assumes that lamellae grow locally normal to the envelope of the eutectic interface. Langer later formalized this result by showing that a large-scale and small-amplitude spacing modulation of a steady-state array obeys the diffusion equation [5]

$$\partial_t \lambda(x,t) = D\, \partial_x^2 \lambda(x,t), \tag{3}$$

where x is the coordinate perpendicular to the growth axis z, and $D = D_\perp$, with

$$D_\perp = \frac{V\lambda_0}{G} \left. \frac{d\Delta T(\lambda)}{d\lambda} \right|_{\lambda=\lambda_0} = \frac{K_1 \lambda_0 V^2}{G} \left(1 - \frac{1}{\Lambda_0^2} \right). \tag{4}$$

We have defined $\Lambda_0 = \lambda_0/\lambda_m$, where λ_0 is the spacing of the steady-state array being perturbed, and we have used the subscript "$\perp$" to stress that this expression for D is obtained under Cahn's assumption that lamellae grow normal to the interface. Langer's analysis reproduces the JH-Cahn result that growth is unstable below λ_m since perturbations are amplified (decay) when $D_\perp < 0$ (> 0). In addition, it shows that

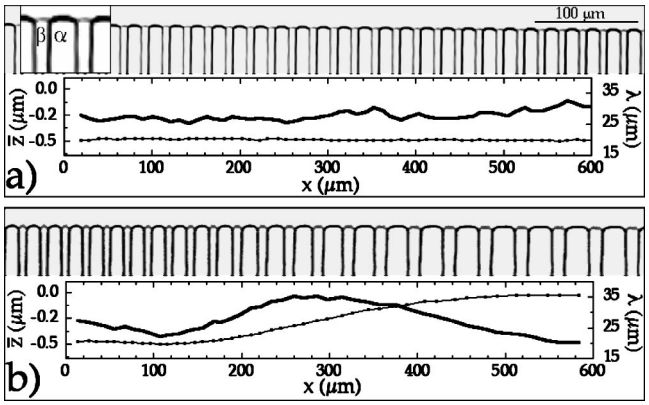

FIG. 1. Photographs: lamellar-eutectic fronts of a nearly eutectic CBr_4-C_2Cl_6 alloy in directional solidification (the growth direction is upward) in 12-μm-thick samples. Graphs show interlamellar spacing λ (thin lines) and position $\bar{z}$ of the front (thick lines) as functions of the space variable x. (a) Stationary pattern ($V = 0.5$ μm s^{-1}, $G = 80$ K cm^{-1}). (b) Modulated pattern ($V = 0.25$ μm s^{-1}, $G = 48$ K cm^{-1}).

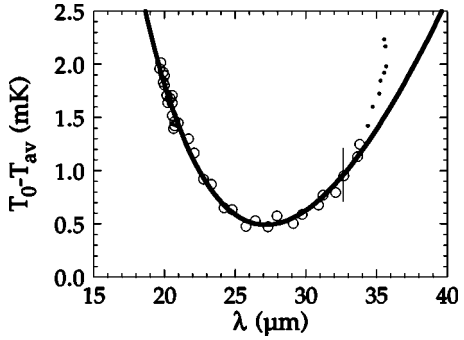

FIG. 2. Undercooling T_0-T_{av} vs spacing λ measured experimentally from the photograph shown in Fig. 1(b) (open circles and dots). The thick line represents the best fit of the JH law, Eq. (1), to the data represented by open circles. The vertical bar represents the error range. A remarkable feature is the presence of spacings considerably smaller than $\lambda_m \approx 27$ μm. The value of the smallest stable spacing λ_c predicted from Eq. (11) below is 19 μm.

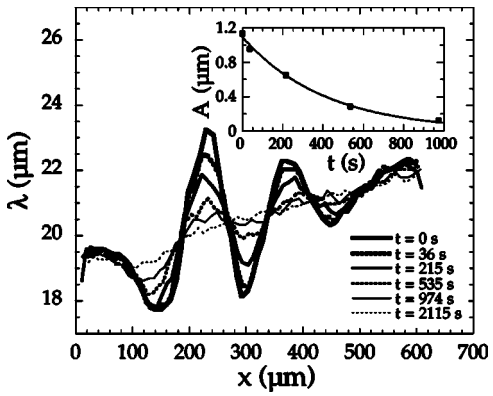

FIG. 3. Experimental measurements of the spacing λ vs the space variable x at different times t showing the relaxation of a large-scale modulation of a lamellar pattern of $\Lambda_0 \approx 1$. ($G = 80$ K cm^{-1}, $V = 0.5$ μm s^{-1}.) The inset shows the amplitude A of the dominant mode (wavelength of 145 μm) as a function of t, fitted by an exponential law (time constant of 410 s).

lamella elimination is initiated by a long-wavelength diffusive instability that is generically present in one-dimensional pattern forming systems with translation symmetry along x.

In this paper, we study the steady-state and stability properties of lamellar eutectic growth by thin-sample directional solidification experiments in the transparent organic system CBr_4-C_2Cl_6 and by two-dimensional simulations of a phase-field model, and we extract from both approaches independent accurate determinations of λ_m and λ_c. An important and novel component of our experiments is the direct measurement of $\Delta T(\lambda)$, which allows us to obtain λ_m from the minimum of this curve rather than computing its value from Eq. (2), thereby circumventing uncertainties in materials parameters. We find that, in both experiments and simulations, λ_c is substantially smaller than λ_m, even for typical directional solidification growth conditions where the two spacings have previously been assumed equal. Furthermore, by analyzing the decay of long-wavelength perturbations of the array in both experiments and simulations, we obtain a direct measurement of D, which allows us to shed light on the origin of the discrepancy between λ_c and λ_m.

The experiments were made with a nearly eutectic CBr_4-C_2Cl_6 alloy prepared with zone refined materials in thin (12-μm-thick) glass wall samples (8 mm wide and 60 mm long). The values of G used ranged from 40 K cm^{-1} to 110 K cm^{-1} ($\pm 10\%$), and those of V from 0.125 to 0.75 μm s^{-1} ($\pm 4\%$). Details concerning the preparation of the samples, the solidification setup, and the visualization of the front shape can be found in Refs. [4,6].

The steady-state $\Delta T(\lambda)$ curve has never been measured directly due to the fact that ΔT_m is usually of the order 0.01 K, whereas the absolute temperature is not known with a precision greater than about 0.1 K. To overcome this difficulty, we exploit two key ingredients. First, as will be described elsewhere, we are able to create a large-scale modulation of spacing where $\lambda(x)$ varies between two extreme values that comprise λ_m, as shown in Fig. 1(b). Second, we measure the z coordinate of the solid-liquid interface averaged over one λ, which we denote by $\overline{z}(x)$, and compute the local front undercooling using $T_{av}(x) = G\overline{z}(x) + T_0$, where T_0 is an unknown constant. By eliminating x between $T_0 - T_{av}(x)$ and $\lambda(x)$, we obtain $T_0 - T_{av}(\lambda)$, which we then fit to Eq. (1) expressed in the form $T_0 - T_{av}(\lambda) = \Delta T_m(\lambda/\lambda_m + \lambda_m/\lambda)/2 - \Delta T_0$, using λ_m, ΔT_m, and $\Delta T_0 = T_E - T_0$ as adjustable parameters. A plot of $T_0 - T_{av}(\lambda)$ and its fit is shown in Fig. 2. The fit is very good for λ lesser than about $1.25\lambda_m$. The departure observed beyond this limit is compatible with the one which exists between the numerically calculated curves $\Delta T(\lambda)$ and the JH approximation [3,7]. We performed such measurements for V ranging from 0.125 to 0.5 μm s^{-1}. We found $\lambda_m^2 V = K_2/K_1 = 193 \pm 16$ μm^3 s^{-1} and $\Delta T_m^2/V = 4K_1K_2 = (2.7 \pm 1.3) \times 10^{-3}$ K^2 s μm^{-1}. These values compare well to those calculated from the material constants of CBr_4-C_2Cl_6 given in Ref. [8], namely, $\lambda_m^2 V = 185 \pm 20$ μm^3 s^{-1} and $\Delta T_m^2/V = (1.2 \pm 0.2) \times 10^{-3}$ K^2 s μm^{-1}.

To study experimentally the small spacing stability limit, we exploit the fact that $\lambda_m \sim V^{-1/2}$. Therefore, we can effectively vary λ_0/λ_m by performing downward velocity jumps of relatively large amplitude. Namely, we start from a stable quasistationary periodic array of spacing λ_0 at a higher velocity, and then observe whether the same array at the lower velocity, and hence smaller λ_0/λ_m, remains stable or becomes unstable.

To measure experimentally the array diffusion constant D, we use the fact that the amplitude of a long-wavelength modulation of spacing of the form

$$\lambda(x,t) \approx \lambda_0 + \delta\lambda_0 \exp(ikx + \omega_k t) \tag{5}$$

decays exponentially in time when the array is stable ($\lambda_0 > \lambda_c$). Substituting this form in Eq. (3), we obtain the simple dispersion relation $\omega_k = -Dk^2$, which is valid if the wavelength of the perturbation $2\pi/k \gg \lambda_0$. Knowing k, and calculating ω_k by a fit of the measured amplitude of the modulation to a decaying exponential, we obtain D. This is illustrated in Fig. 3 for a case where $2\pi/k \approx 7\lambda_0$. We deduce

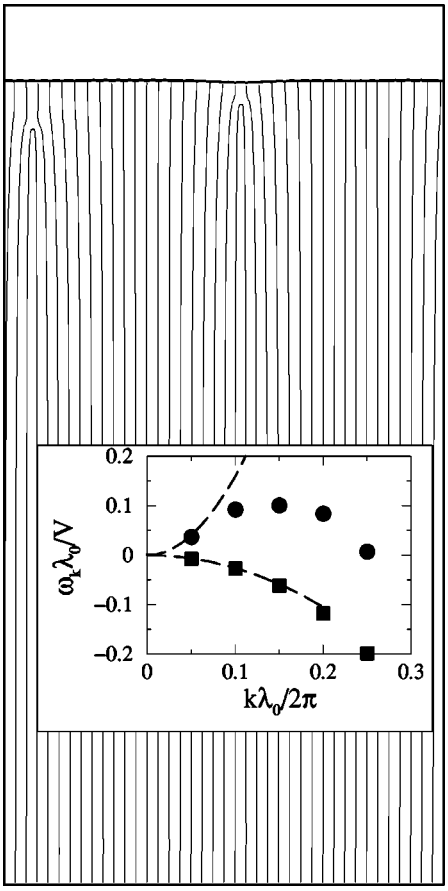

FIG. 4. Simulated evolution of an unstable array for $\Lambda_0=0.84$ and $l_T/l_D=20$. Growth direction is from bottom to top. For a ten times larger temperature gradient ($l_T/l_D=2$), the same array was stable, although Λ_0 is significantly smaller than 1. The inset shows growth rates ω_k of spacing perturbations versus wave vector k. Circles represent $l_T/l_D=20$; squares represent $l_T/l_D=2$. Dashed lines represent the fits $\omega_k=Dk^2$, obtained from the points with smallest k.

from this measurement that

$$D=D_\perp+D_\parallel, \tag{6}$$

where $D_\parallel$ is a positive contribution responsible for the overstabilization of the array. The latter is calculated by taking the difference between D, and $D_\perp$ evaluated via Eq. (4) using the value $K_1=1.9\times10^{-3}$ K s μm^{-2} obtained from our present experiments.

Next, we simulate a simple phase-field model of a two-component (AB) eutectic alloy that is completely symmetric under the exchange of α and β [9]. Our goal here is not to model quantitatively the experiments but to demonstrate the generality of our results in different alloy systems. The model works with two dynamic fields, an order parameter ϕ that distinguishes between liquid and solid, and the concentration c (mole fraction of B). The solute diffusivity vanishes in the solid and is constant and equal to D_l in the liquid. Directional growth is implemented using the frozen-temperature approximation $T(z,t)=T_E+Gz-Vt$, and periodic boundary conditions in x are used in all simulations

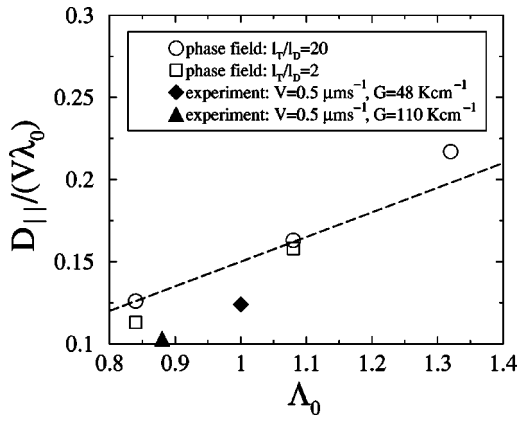

FIG. 5. $D_\parallel/(V\lambda_0)$ vs Λ_0 for simulations and experiments. Dashed line, Eq. (7) drawn with $A=0.15$.

[10]. The strength of the temperature gradient is measured by the ratio l_T/l_D, where $l_T=m\Delta c/G$ is the thermal length (m is the magnitude of the liquidus slope in the phase diagram and Δc is the width of the eutectic plateau) and $l_D=D_l/V$ is the diffusion length.

Steady-state $\Delta T(\lambda)$ curves were obtained from short simulations with two lamellae. The stability was studied with long simulations where steady-state arrays of up to 20 lamellae, constructed from the two-lamella solutions, are slightly perturbed by a small random modulation of the spacing (Fig. 4). The stability spectrum is obtained from a Fourier decomposition of the trijunction positions and exponential fits of the amplitude of modulation vs time for different wave numbers k. Next, D is extracted by a quadratic fit of ω vs k at small k. The stability limit λ_c is then obtained by determining where D changes sign, and the values of $D_\parallel$ are obtained by subtracting $D_\perp$ from D. We find that the dimensionless ratio $D_\parallel/(V\lambda_0)$ varies with Λ_0, but negligibly with G and V. Moreover, we find that the simple form

$$D_\parallel/(V\lambda_0)\approx A\Lambda_0 \tag{7}$$

with $A\approx0.15$ gives a reasonable fit to our phase-field simulation results as shown in Fig. 5. Remarkably, our experimentally determined values of $D_\parallel$ are close to those obtained in the phase-field simulations, even though the two alloy systems are different.

To interpret our findings, let us briefly review Langer's analysis that yields $D=D_\perp$. Its first ingredient is the assumption that the interface adjusts adiabatically its average temperature to the local spacing, or

$$\Delta T(\lambda(x,t))\approx -G\zeta(x,t), \tag{8}$$

where $\Delta T(\lambda)$ is the same as in steady state and $\zeta(x)$ is the z coordinate of the envelope of the eutectic interface, defined as a smooth curve interpolating the positions of the three-phase junctions (trijunctions), with the origin at T_E. The second is Cahn's assumption that lamellae grow normal to this envelope, which for a small perturbation is equivalent to

$$\partial_t y(x,t)\approx -V\partial_x\zeta(x,t), \tag{9}$$

where $y(x,t)$ is the lateral displacement of trijunctions from their steady-state positions. Finally, it follows from the definition of y that $\lambda(x,t) \approx \lambda_0(1+\partial_x y)$. Differentiating both sides of this identity with respect to time and using Eqs. (1), (8), and (9), one obtains the diffusion equation (3) with $D = D_\perp$.

We checked that Eq. (8) is indeed faithfully obeyed in the range of wavelengths that we consider here. Consequently, the discrepancy between D and $D_\perp$ must originate from a correction to Cahn's normal growth assumption. It is simple to show that the modified phenomenological form

$$\partial_t y(x,t) \approx -V\partial_x \zeta(x,t) + D_\parallel \partial_x \lambda(x,t)/\lambda_0 \qquad (10)$$

yields the diffusion equation (3), with D given by Eq. (6). Equation (10) implies that trijunctions also move locally ''parallel'' to the envelope of the eutectic interface in response to a gradient of spacing. To see physically why this lateral motion overstabilizes the pattern, consider a local depression in an array of initial spacing λ_0. Cahn's normal growth assumption implies that such a depression will produce a local decrease of spacing, and hence a local increase in undercooling will amplify this depression if $\lambda_0 < \lambda_m$ (because $d\Delta T/d\lambda < 0$ in this case). This well-known argument yields $\lambda_c = \lambda_m$. In contrast, the second term on the right-hand side of Eq. (10) implies that the lateral motion of trijunctions opposes the local decrease in λ, and hence helps flatten the interface.

A prediction for $\Lambda_c = \lambda_c/\lambda_m$ can be obtained by setting $D = D_\perp + D_\parallel = 0$, which, using Eqs. (2), (4), and (7), yields the cubic equation

$$1 - \frac{1}{\Lambda_c^2} + \frac{AG}{K_1 V}\Lambda_c = 0. \qquad (11)$$

With $K_1 = 1.9\times 10^{-3}$ K s μm^{-2} and $A = 0.15$, we obtain $\Lambda_c = 0.70$ for the experiment of Fig. 2; the lowest observed spacings are just above the predicted stability threshold, as it should be. For the phase-field simulations ($K_1 = 0.1120$), we find $\Lambda_c = 0.942$ for $l_T/l_D = 20$ and $\Lambda_c = 0.715$ for $l_T/l_D = 2$.

Two previous stability analyses have predicted that λ_c should be smaller than λ_m. The one by Caroli and coworkers [11], however, is restricted to a large G limit that cannot be compared with our results. The other by Chen and Davis [12] does not have this restriction, but predicts a departure of λ_c from λ_m that is about one order of magnitude smaller than found here and predicted by Eq. (11). We believe that the lateral motion of the trijunctions is due to a coupling between the diffusion field and the nonplanar front geometry on the scale of the individual lamellae; such effects would appear only at higher orders in the analyses cited above. Therefore, an analytical understanding of eutectic stability at small spacings from sharp-interface models is still lacking.

The present results shed light on a number of previous observations. In metallic eutectics, K_1 is generally close to 10^{-2} K s μm^{-2} [13,14], so that the value of V below which the departure of Λ_c from unity becomes significant is of about 1 μm s^{-1} for G in the 100 K cm^{-1} range. This may explain the deviation from the law $\bar{\lambda} \propto V^{-0.5}$, where $\bar{\lambda}$ is some empirically defined average eutectic spacing, which has been observed at V lower than about 1 μm s^{-1} in a number of metallic eutectics [15]. Similarly, the overstability due to the lateral motion of the trijunctions may explain why coupled growth in a peritectic system has recently been found to be stable [16] in a situation, analogous to that of eutectics at $\lambda < \lambda_m$, where the interface should be unstable according to the JH-Cahn stability arguments [17]. Finally, our results also improve our understanding of the morphological instability that leads to the formation of eutectic colonies in the presence of a dilute ternary impurity [6,9].

This work was supported by the Centre National d'Etudes Spatiales, France, and by the US Department of Energy under Grant No. DE-FG02-92ER45471.

[1] W.Kurz and D.J. Fisher, *Fundamentals of Solidification* (Trans Tech, Aedermannsdorf, Switzerland, 1992).

[2] K.A. Jackson and J.D. Hunt, Trans. Metall. Soc. AIME **236**, 1129 (1966).

[3] A. Karma and A. Sarkissian, Met. Trans. A **27**, 635 (1996); A. Sarkissian, Ph.D. thesis, Northeastern University, Boston, 1996.

[4] M. Ginibre, S. Akamatsu, and G. Faivre, Phys. Rev. E **56**, 780 (1997).

[5] J.S. Langer, Phys. Rev. Lett. **44**, 1023 (1980).

[6] S. Akamatsu and G. Faivre, Phys. Rev. E **61**, 3757 (2000).

[7] K. Kassner and C. Misbah, Phys. Rev. A **44**, 6513 (1991).

[8] J. Mergy, G. Faivre, C. Guthmann, and R. Mellet, J. Cryst. Growth **134**, 353 (1993).

[9] M. Plapp and A. Karma, e-print cond-mat/0112194.

[10] In the notations of Ref. [9], the simulation parameters are $W_u = W_\phi = D_l = \tau = T_E = 1$, $a = 1/8$, $n = 4$, $V = 0.01$, $\Delta x = 1$, $\Delta t = 0.025$; the resulting minimum undercooling spacing is $\lambda_m = 33.3$.

[11] K. Brattkus, B. Caroli, C. Caroli, and B. Roulet, J. Phys. (France) **51**, 1847 (1990); B. Caroli, C. Caroli, and B. Roulet, *ibid.* **51**, 1865 (1990).

[12] Y.-J. Chen and S.H. Davis, Acta Mater. **49**, 1363 (2001).

[13] M. Gündüz and J.D. Hunt, Acta Metall. **33**, 1651 (1985).

[14] R. Trivedi, J.T. Mason, J.D. Verhoeven, and W. Kurz, Metall. Trans. A **22A**, 252 (1991).

[15] R. Racek, G. Lesoult, and M. Turpin, J. Cryst. Growth **22**, 210 (1974).

[16] M. Vandyoussefi, H.W. Kerr, and W. Kurz, Acta Mater. **45**, 4093 (1997); S. Dobler *et al.* (unpublished).

[17] W.J. Boettinger, Metall. Trans. **5**, 2023 (1974).